Purdue University
Purdue e-Pubs

International Compressor Engineering Conference

School of Mechanical Engineering

1980

Computer Simulation of a Reciprocating Compressor Using a Real Gas Equation of State

E. H. Ng

A. B. Tramschek

J. F. T. MacLaren

COMPUTER SIMULATION OF A RECIPROCATING COMPRESSOR USING A REAL GAS EQUATION OF STATE

E H Ng, Research Student
A B Tramschek, Lecturer
J F T MacLaren, Professor

Department of Thermodynamics & Fluid Mechanics

University of Strathclyde, Glasgow

ABSTRACT

A model is described which may be used to simulate the events in a reciprocating compressor when the thermodynamic properties of the working fluid are represented by a real gas equation of state. A comparison is made between calculated parameters of performance obtained using the Martin-Downing form of the equation of state for refrigerant R12 and corresponding results obtained using a similar analysis in which the state of the working fluid is described by the ideal gas equation.

Results from a typical reciprocating compressor are reported for many of the parameters of interest to the designer eg p-V and valve displacement diagrams, mass flow rates, volumetric efficiency, cycle work, various losses etc. Use of the real gas equation of state in the simulation model was only justified if at inlet to the compressor the refrigerant had little superheat and the compressor pressure ratio was large.

INTRODUCTION

Mathematical simulation of the behaviour of reciprocating compressors, compressor valves and the working fluid has been under development since 1950 (1): the complexity of the models has increased in order to simulate more closely the actual events in the compressor. Most models (2,3,4) have been developed using the ideal gas equation of state for the thermodynamic properties of the working fluid. Since errors of some unknown magnitude arise if the simple ideal gas equation is used instead of more complex but exact real gas equations,an attempt has been made to quantify such errors by use of simulation model in which either real gas or ideal gas equation of state could be used. The Martin-Downing form of real gas equation (5) was used in this investigation (Appendix B). The thermodynamic properties of several Freon refrigerants obtained by using this formulation were available as a subroutine to a main program which described the events in a compressor cycle. Such subroutines for properties of real fluids are now generally available but, apart from the investigation by Röttger (6), there is little information on whether inclusion of them in compressor simulation models justifies the additional computer time or capacity required.

In the simulation model used in this investigation a number of simplifying assumptions were made. It was assumed that the inlet and discharge receivers were so large that the plenum chamber pressures ps and pd, Figure 1, remained constant, that the heat transfer inside the cylinder was negligible, and that the mass flow through the valves was one-dimensional, with constant flow and force coefficients. The first assumption is avoided in the more advanced models available (7,8) but was retained in the present study in order to focus attention on differences arising solely from the use of different equations to describe fluid properties.

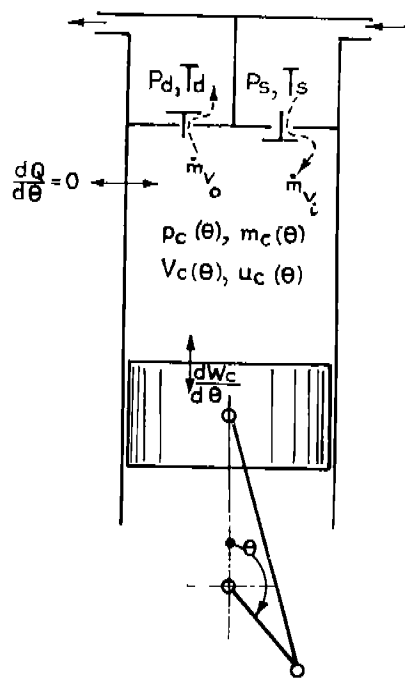

FIG. 1. CYLINDER AND VALVE THERMODYNAMICS.

THE MATHEMATICAL MODEL

Energy Equation for the Cylinder Contents

Taking the cylinder enclosure (Figure 1) as the boundary of the control volume, the energy equation for the cylinder contents can be written as:

$$\frac{dQ_c}{dt} + \Sigma \frac{dm_i}{dt} (h_i + \frac{\bar{V}_i^2}{2} + z_i g) =$$

$$\frac{dW_c}{dt} + \Sigma \frac{dm_o}{dt} (h_o + \frac{\bar{V}_o^2}{2} + z_o g) + \frac{d}{dt} (m_c u_c) \quad \dots\dots (1)$$

The work term can be written as:

$$\frac{dW_c}{dt} = p_c \frac{dV_c}{dt} \quad \dots\dots\dots\dots\dots\dots\dots\dots\dots (2)$$

Differentiating the internal energy term and applying the definition of enthalpy,

$$h = u + pv \quad \dots\dots\dots\dots\dots\dots\dots\dots\dots\dots (3a)$$

and the mass equation $v_c = \frac{V_c}{m_c}$ .... (3b)

then $\frac{d}{dt} (m_c u_c) =$

$$m_c \frac{dh_c}{dt} - p_c \frac{dV_c}{dt} - V_c \frac{dp_c}{dt} + h_c \frac{dm_c}{dt} \quad \dots\dots\dots\dots (4)$$

The potential and kinetic energy terms, relatively small compared to the internal energy and enthalpy terms, may be neglected. Heat transfer inside the cylinder is also neglected on the assumption that adiabatic processes are occurring. Substituting equations (2) and (4) into equation (1) gives

$$\frac{dh_c}{d\theta} =$$

$$\frac{1}{m_c} [\Sigma \frac{dm_i}{d\theta} (h_i - h_c) - \Sigma \frac{dm_o}{d\theta} (h_o - h_c) + V_c \frac{dp_c}{d\theta}] \quad \dots\dots (5)$$

where the equation now takes the rate form in terms of crank angle.

Now, let h = (T,v)

and $$\frac{dh}{d\theta} = (\frac{\partial h}{\partial T})_v \frac{dT}{d\theta} + (\frac{\partial h}{\partial v})_T \frac{dv}{d\theta} \quad \dots\dots\dots\dots\dots\dots (6)$$

Equating equations (5) and (6) gives,

$$\frac{dp_c}{d\theta} =$$

$$\frac{1}{v_c} [(\frac{\partial h_c}{\partial T_c})_v \frac{dT_c}{d\theta} + (\frac{\partial h_c}{\partial v_c})_T \frac{dv_c}{d\theta}] - \frac{1}{V_c} [\Sigma \frac{dm_i}{d\theta} (h_i - h_c) +$$

$$\Sigma \frac{dm_o}{d\theta} (h_o - h_c)] \quad \dots\dots\dots\dots\dots\dots\dots (7)$$

The two unknowns involved in equation (7) are the pressure and temperature of the contents of the cylinder. The partial derivatives and the enthalpies are determined from the refrigerant property subroutine using the real gas equation of state, while $\frac{dv_c}{d\theta}$ is determined from the mass equation.

To solve for p and T, a second relationship between pressure and temperature is needed, and is obtained from p = p(T,v)

hence $$\frac{dp_c}{d\theta} = \left(\frac{\partial p_c}{\partial T_c}\right)_v \frac{dT_c}{d\theta} + (\frac{\partial p_c}{\partial v_c})_T \frac{dv_c}{d\theta} \quad \dots\dots\dots\dots\dots (8)$$

Again, the partial derivatives are determined from the real refrigerant property subroutine. Equations (7) and (8) form two simultaneous first order differential equations with p and T as unknowns. These two unknowns can be solved for at intervals of crank angle, $\Delta\theta$, by numerical integration of equations (7) and (8).

The Mass Equation

The mass of fluid inside the cylinder is

$$m_c (\theta) = \frac{V_c}{v_c} \quad \dots\dots\dots\dots\dots\dots\dots\dots\dots\dots (9)$$

and $$\frac{dv_c}{d\theta} = \frac{1}{m_c} \frac{dV_c}{d\theta} - \frac{V_c}{m_c^2} \frac{dm_c}{d\theta} \quad \dots\dots\dots\dots\dots\dots (10)$$

where $\frac{dV_c}{d\theta}$ can be determined since the cylinder volume is a function of crank angle measured from top dead centre; $\frac{dm_c}{d\theta}$ is the difference between the mass flow rate of fluid into and out of the cylinder.

Mass Flow Through Valves

The equation for one-dimensional adiabatic flow through a valve may be written as

$$\frac{dm_v}{d\theta} = \frac{C_d \alpha A_o}{\omega v_2} \sqrt{2 (h_1 - h_2) + \bar{V}_1^2} \quad \dots\dots\dots\dots\dots (11)$$

where suffixes 1 and 2 denote the condition of the fluid upstream and downstream of the valve respectively. The kinetic energy term can be neglected since it is very small compared to the enthalpy term. The product αA_o is the valve flow area, which is a function of valve lift.

Dynamic Equation for Valve Movement

Assuming one degree of freedom for the spring-mass system, the equation of valve motion is,

$$M \frac{d^2y}{dt^2} + R \frac{dy}{dt} + k \ y + \lambda = C_D A_V \Delta p \text{ .... } (12)$$

Equation (12) may be expressed non dimensionally and in terms of crank angle using the relationship $\theta = \omega t$ .... (13)

(When the valves are closed equations (7) and (8) alone are integrated simultaneously, however, if the valves are moving equations (7), (8) and (15) are integrated simultaneously). Introducing $\alpha = \frac{y}{y_o}$, the dynamic equation in terms of crank angle can be re-written as:

$$\frac{d^2\alpha}{d\theta^2} = \frac{C_D A_V \Delta p}{M\omega^2 y_o} - \frac{R}{M\omega}\frac{d\alpha}{d\theta} - \frac{k\alpha}{M\omega^2} - \frac{\lambda}{M\omega^2 y_o} \text{ .... } (14)$$

or letting $\omega^2_n = \frac{k}{M}$ and $F = \frac{\omega}{\omega_n}$

$$\frac{d^2\alpha}{d\theta^2} = \left(\frac{C_D A_V \Delta p}{F^2 k\ y_o}\right) - \frac{R\omega_n}{kF}\frac{d\alpha}{d\theta} - \frac{\alpha}{F^2} - \frac{\lambda}{F^2 k y_o} \text{ .... } (15)$$

$\Delta p = Ps - Pc$ for the suction valve

and $\Delta p = Pc - Pd$ for the discharge valve

Equation (15) is a second order differential equation which can be reduced to two simultaneous first order differential equations and integrated numerically at small intervals of crank angle using the Kutta-Merson procedure.

OUTLINE OF THE COMPUTER PROGRAMS

A computer program was written to calculate the conditions in a compressor cycle using small increments of crank angle ($\Delta\theta$). The program is initialised at starting point 0 (Figure 2). At point 0 it is assumed that $\theta = 0°$, the cylinder pressure is equal to the nominal discharge pressure p_d, while the cylinder temperature T_c, is obtained from the relevant p-h chart by assuming that compression is isentropic from the nominal suction conditions temperature T_s, pressure p_s to the discharge pressure. Equations (7) and (8) are solved by the Kutta-Merson procedure, over the small increment of crank angle, to predict the next values of p_c and T_c.

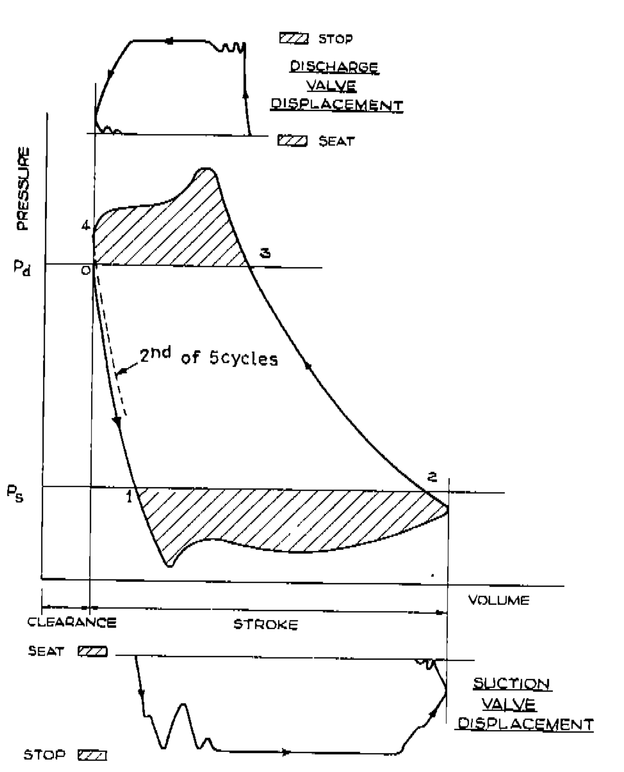

FIG 2.
PRESSURE - VOLUME AND VALVE DISPLACEMENT DIAGRAMS

At each crank angle, the cylinder pressure p_c and temperature T_c are now known hence, by using the Martin-Downing equation of state, the other properties such as specific enthalpy, specific entropy and eventually specific volume can be obtained, together with their partial derivatives. The cylinder volume is calculated at each crank angle and knowing the appropriate value of specific volume, the cylinder mass can be calculated. from equation (9). (Having calculated the variation of p_c and T_c during the re-expansion process an index of expansion can be calculated, if desired, which relates the initial and final gas states: this index cannot be used to predict any intermediate conditions between the end state points. Similarly, an index of compression can be deduced which relates the end state points on the compression curve from point 2 to point 3, Figure 2.) During opening and closing of the suction or discharge valve, the dynamic equation (15) is solved to obtain the valve lift and the corresponding valve velocity.

After completion of the first compressor cycle, the discharge valve may not close at point 0, so the original assumptions about conditions at point 0 may be in error. The cycle was recalculated five times, revising the initial conditions at point 0 after each cycle, to ensure that adequate convergence had been achieved. After the fifth cycle, several parameters are calculated, including the total cycle work, various losses of power and capacity, the actual, indicated and theoretical volumetric efficiencies, the actual and theoretical mass flows, the corresponding performance ratios, and the ratio of the performance ratios as defined in Appendix A.

A second program employed the ideal gas equation. This program is identical to the program using the Martin-Downing equation of state except that all the constants in the equation are set equal to zero. Both programs create files in the computer during the computation of the fifth cycle so that results, such as the p-V and valve displacement diagrams, can be graphed (Figure 8).

The step sizes used in the model were 0.5° crank angle when a valve was opening or closing and 1° crank angle when a valve was at rest against either its stop or seat. Hence the equations were solved about 415 times during each compressor cycle, with 230 to 260 calculations during a suction process and 41 to 66 during a discharge process. The cycle (Figure 2) was completed 5 times during each test cited in Table I to ensure convergence prior to print out of results. The time required for a test was about 5 minutes on an ICL 1904S computer. There was negligible difference in time whether the real or ideal gas equation was used because when using the ideal gas equation the constants in the real gas equation were included as zeros (Appendix B).

The present model calculates conditions at small intervals of crank angle during a cycle. An index of compression or re-expansion (Table I) can be deduced later which links the state of the gas at the beginning and end of these processes. The model developed by Kerr (2), based on that by Costagliola (9) uses the simple ideal gas equation and considers the cycle to consist of four discrete phases: re-expansion and compression (which employ appropriate indices as empirical coefficients) and the suction and discharge phases. Only these last two phases require the time consuming step-by-step integration procedures. The same compressor dimensions and operating conditions were used as input data to the Kerr model and the computer time required was only about one minute. Hence when the gas is highly superheated, as in hermetic and semi-hermetic compressors, a saving in computer time can be achieved and adequate results obtained providing appropriate indices of re-expansion and compression are used.

Application of the Model

The model was applied to a 7.5 h.p., 3 cylinder semi-hermetic compressor with cylinder bore 2.491 in, piston stroke 2.5 in, speed 1450 rev/min, fitted with reed type suction and discharge valves. Refrigerant R12 was used at one evaporator pressure (9.3 lbf/in^2 abs) and temperature (-40°F) with three suction temperatures at increasing order of superheat (10, 60, 120 F deg superheat) and 5 compressor pressure ratios (4, 8, 10, 12, 14).

Values of some of the various parameters predicted by the model for the range of conditions are listed in Table I for both the real gas and ideal gas cases. The difference between the results for

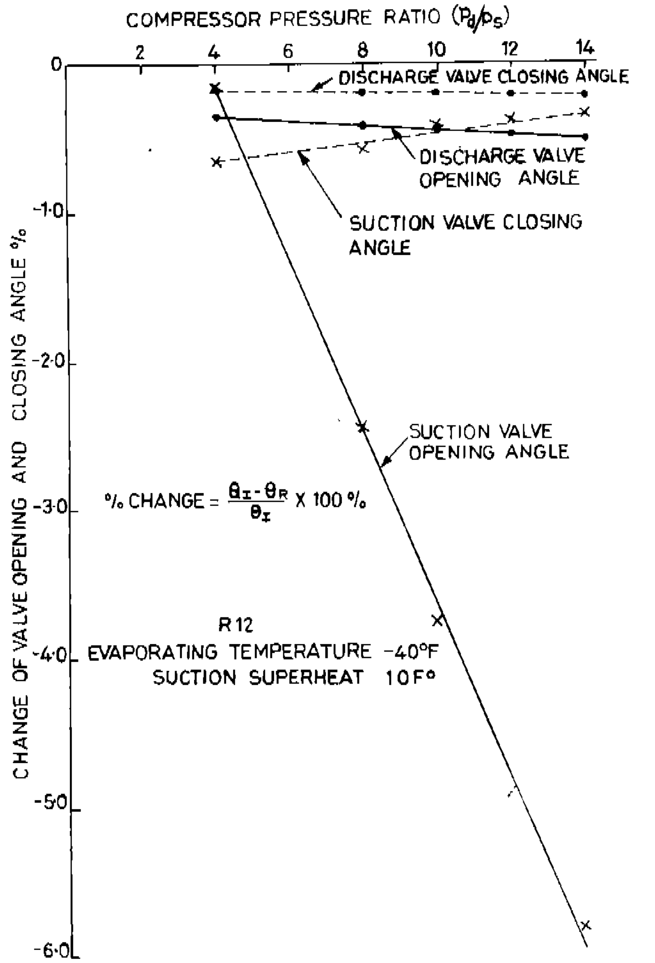

FIG 3. PERCENTAGE CHANGE OF VALVE OPENING AND CLOSING ANGLES.

the two cases for a selection of the parameters are shown in Figures 3, 4, 5, 6 and 7. Two of the parameters, volumetric efficiency and ratio of performance ratios, are discussed in Appendix A. Figure 8 is a sample of the graphical output by the computer (for Test 2, Table I) of the p-V diagram, the mass of gas in the cylinder and its temperature during the cycle, the pressure difference across the suction and discharge valves and the displacement of each valve with respect to crank angle.

Figures 3 and 4 record the effect of introducing the real gas equation when computing the crank-angle at which valves open and close and the veloctiy of valve impact at seat and stop. Figures 5, 6, 7 show the effect on important parameters relating to compressor performance when these parameters were evaluated using the real gas equation. Figure 5 which records a criterion of overall performance (RPR, Appendix A) illustrates that divergence from the values when employing the ideal gas equation was greater if the state of the gas was nearer to the saturation condition. This was expected since the gas behaves less ideally at low values of superheat. The model incorporating the real gas equation predicted lower total cycle work and lower ideal cycle work but higher values of

TABLE I - TEST RESULTS	TEST 1		TEST 2		TEST 3		TEST 4		TEST 5	
	REAL	IDEAL	REAL	IDEAL	REAL	IDEAL	REAL	IDEAL	REAL	IDEAL
Speed (rev/min)	1450	1450	1450	1450	1450	1450	1450	1450	1450	1450
Evaporating Pressure (psia)	9.3	9.3	9.3	9.3	9.3	9.3	9.3	9.3	9.3	9.3
Discharge Pressure (psia)	37.2	37.2	74.4	74.4	93.0	93.0	111.6	111.6	130.2	130.2
Compressor Pressure Ratio	4	4	8	8	10	10	12	12	14	14
Suction Temperature (°F)	-30	-30	-30	-30	-30	-30	-30	-30	-30	-30
Evaporating Temperature (°F)	-40	-40	-40	-40	-40	-40	-40	-40	-40	-40
Suction Valve Opens (deg)	24.92	24.88	36.21	35.35	41.07	39.59	45.73	43.60	50.23	47.47
Suction Valve Impact Velocity at Stop (ft/s)	19.54	19.57	18.61	18.71	18.21	18.36	17.84	18.03	17.49	17.71
Suction Valve Closes (deg)	251.8	250.2	250.6	249.2	249.5	248.4	248.0	247.1	246.4	245.5
Suction Valve Impact Velocity at Seat (ft/s)	10.51	10.39	10.43	10.33	10.32	10.28	10.21	10.16	10.06	10.03
Expansion Index	1.121	1.142	1.119	1.147	1.115	1.146	1.110	1.144	1.105	1.143
Actual Cycle Work (ft lbf)	17.47	17.79	20.53	21.28	21.29	22.23	21.78	23.00	22.07	23.60
Theoretical Cycle Work (ft lbf)	12.67	12.86	18.15	18.83	19.53	20.49	20.44	21.71	21.00	22.61
Suction Work (ft lbf)	4.00	3.97	3.67	3.68	3.45	3.51	3.22	3.32	2.98	3.11
Suction Work/Theo Cycle Work (%)	31.56	30.85	20.20	19.56	17.67	17.14	15.73	15.27	14.20	13.75
Actual Volumetric Efficiency 1 (%)	70.49	71.61	66.75	68.06	65.16	66.55	63.68	65.39	62.15	64.23
Indicated Volumetric Efficiency (%)	77.79	78.79	73.47	74.74	71.51	72.94	69.64	71.43	67.70	69.92
Blowby Loss (%)	1.71	1.72	1.61	1.62	1.53	1.55	1.46	1.46	1.35	1.37
Throttling Loss (%)	5.15	5.11	4.72	4.75	4.45	4.53	4.14	4.27	3.84	4.01
Actual Volumetric Efficiency 2 (%)	70.93	71.96	67.14	68.37	65.53	66.86	64.04	65.70	62.51	64.54
Theoretical Volumetric Efficiency (%)	92.79	92.79	84.17	84.17	80.06	80.06	76.06	76.06	72.13	72.13
Discharge Valve opens (deg)	316.0	314.9	330.4	329.0	334.1	332.7	336.9	385.3	339.1	337.3
Discharge Valve Impact Velocity at stop (ft/s)	26.25	26.33	38.15	38.47	42.42	42.86	45.98	46.58	49.12	49.88
Discharge Valve Closes (deg)	359.4	358.7	360.8	360.2	361.4	360.7	362.1	361.3	362.6	361.8
Discharge Valve Impact Velocity at seat (ft/s)	12.41	11.77	12.71	11.69	12.99	12.00	13.46	12.54	13.92	12.93
Compression Index	1.085	1.108	1.070	1.104	1.066	1.104	1.063	1.104	1.060	1.105
Discharge Work (ft lbf)	3.31	3.42	2.15	2.30	1.86	2.00	1.67	1.83	1.53	1.72
Discharge Work/Theo Cycle Work (%)	26.14	26.58	11.87	12.21	9.54	9.77	8.18	8.41	7.29	7.59
Cylinder Mass Induced (lbm) (x 10^3)	1.198	1.181	1.134	1.122	1.107	1.097	1.082	1.078	1.056	1.059
Actual Mass Flow (lbm/hr)	314.6	309.7	297.8	294.3	290.7	287.8	284.1	282.8	277.2	277.8
Actual Performance Ratio (lbm/hp hr)	358.4	348.1	282.8	269.9	266.2	251.8	255.3	239.7	247.2	230.4
Theoretical Mass Flow (lbm/hr)	411.6	399.4	373.3	362.3	355.1	344.6	337.3	327.3	319.9	310.4
Theoretical Performance Ratio (lbm/hp hr)	739.4	706.6	468.2	437.8	413.7	382.7	375.6	343.1	346.6	312.5
Ratio of Performance Ratios (RPR)	0.485	0.493	0.604	0.617	0.643	0.658	0.680	0.698	0.713	0.738
Change of RPR (%)	1.614		2.037		2.210		2.703		3.287	

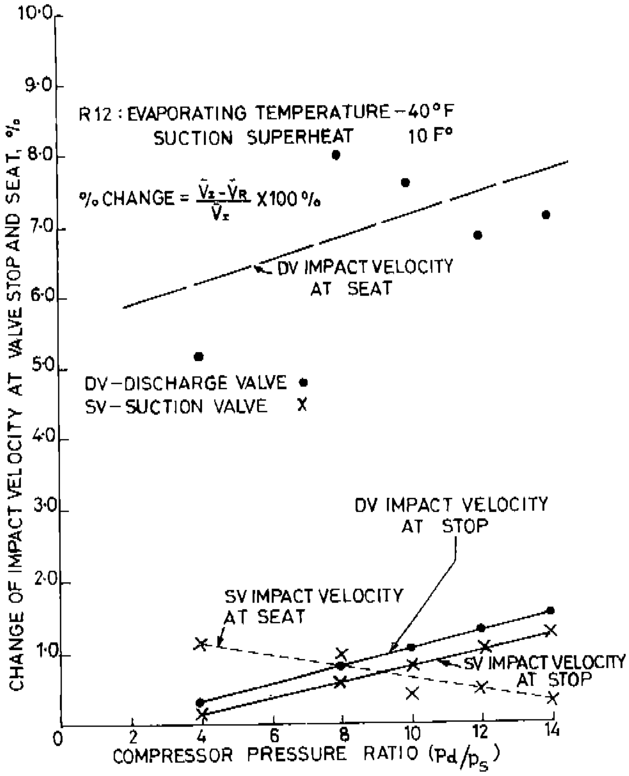

FIG. 4. PERCENTAGE CHANGE OF VALVE IMPACT VELOCITY AT STOP AND SEAT.

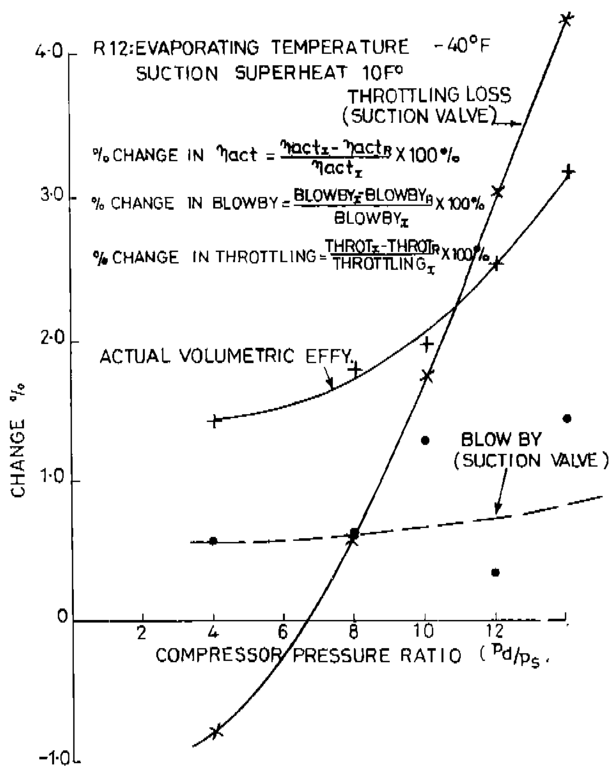

FIG. 7 PERCENTAGE CHANGE OF ACTUAL VOLUMETRIC EFFICIENCY, VALVE BLOW BY AND THROTTLING.

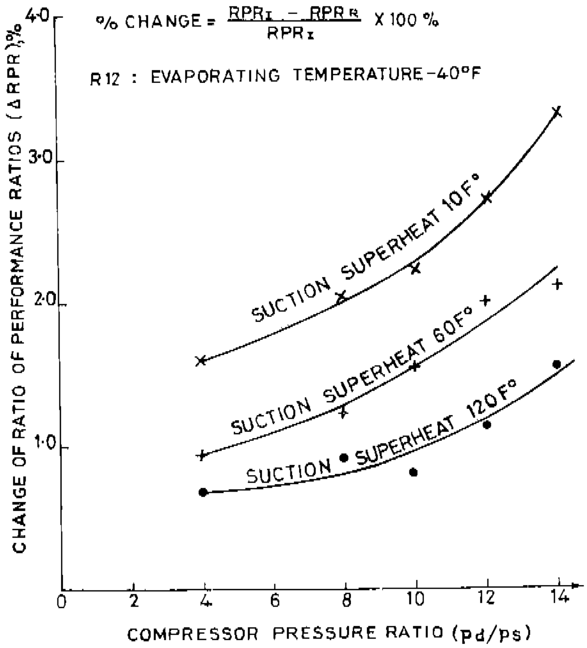

FIG. 5. PERCENTAGE CHANGE OF RATIO OF PERFORMANCE RATIOS

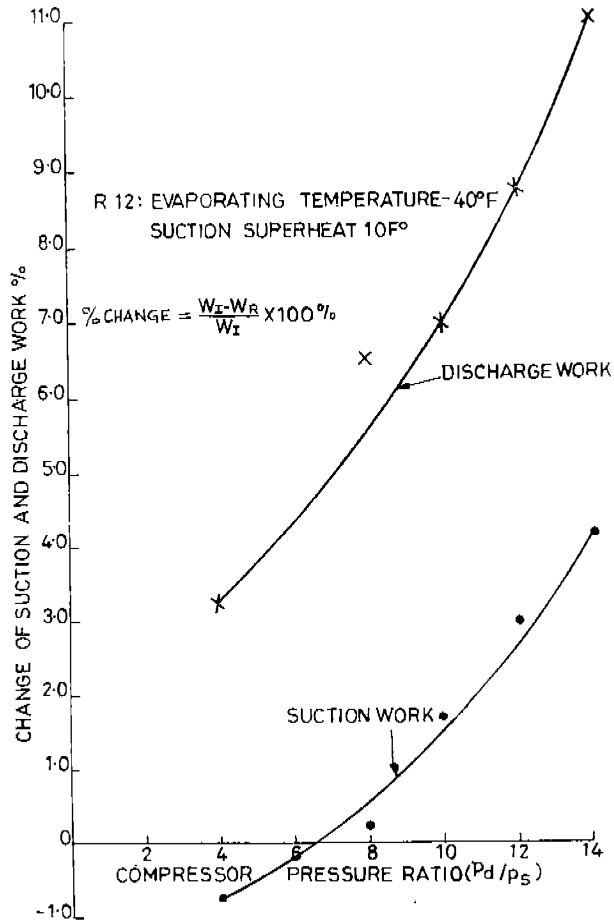

FIG 6. PERCENTAGE CHANGE OF SUCTION AND DISCHARGE WORK.

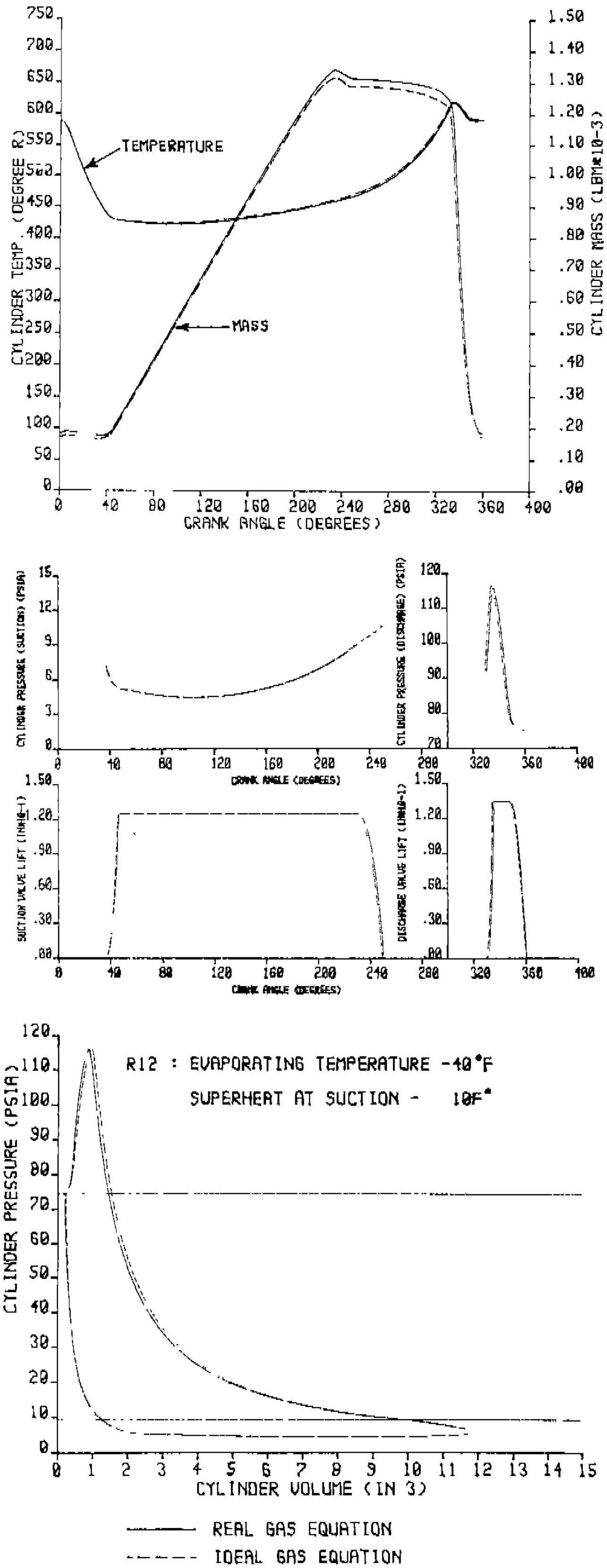

FIG.8 PREDICTIONS BY SIMULATION MODEL (NG)

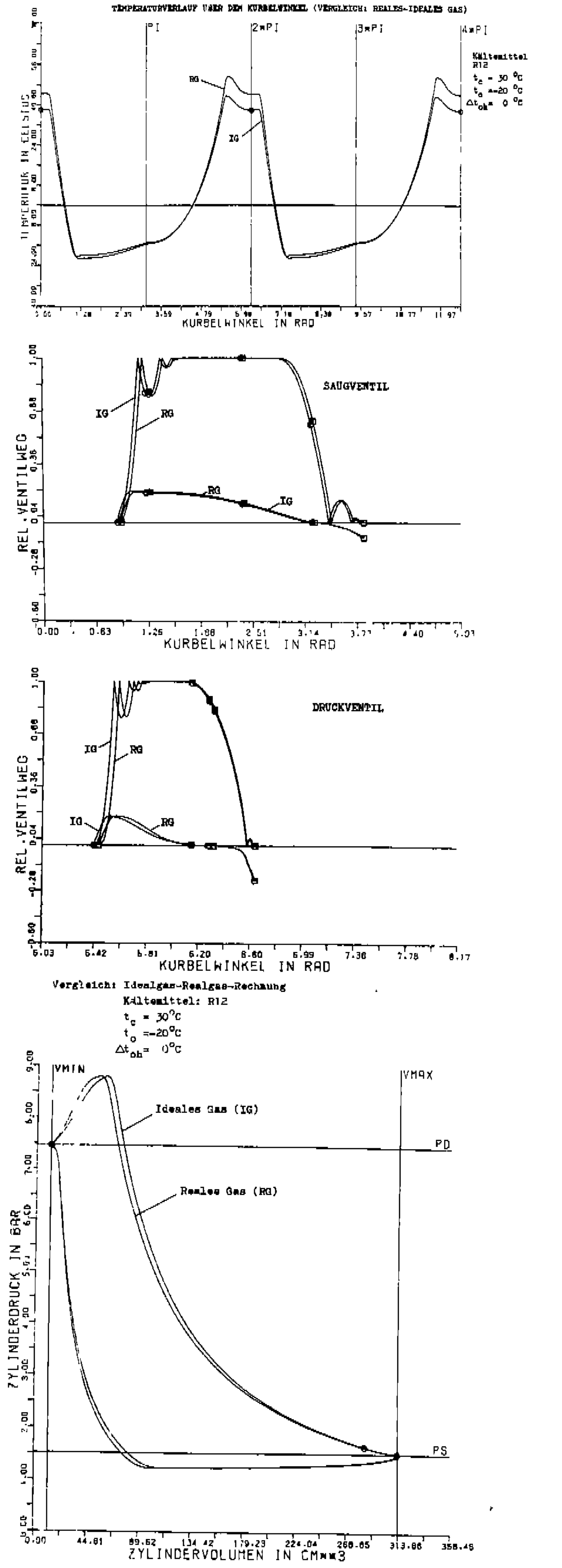

FIG. 9. PREDICTIONS BY SIMULATION MODEL (RÖTTGER)

total cycle (actual) and ideal (theoretical) flow rates (Table I). The net effect was that both the actual and theoretical performance ratios (the ratio of mass flow rate to cycle power) were higher when the real gas equation was used. In the case with low superheat at suction (10 F deg superheat) and high compressor pressure ratio (14) the theoretical performance ratio was increased by almost 10% by using the real gas equation. Table I also shows that the work done during suction as a percentage of the theoretical cycle work tended to be greater when the real gas equation was used. The opposite was the case during the discharge part of the cycle.

Consideration of the parameters in Figure 6 and 7 (the work done in overcoming the resistance of the suction and discharge valves, the actual volumetric efficiency, the suction valve blow-by loss and the loss of capacity due to throttling across the suction valve) show that the divergence when using the real gas equation increased as the compressor pressure ratio increased, even although the evaporator pressure and suction temperature had been held constant.

While Figures 3, 4, 5, 6, and 7 record the difference between various parameters of interest to the designer as a consequence of employing the real gas equation, Figure 8 records the abosolute values of some quantities when both the real and ideal gas equations were used. Presentation of results in this form demonstrates more that the differences were not large. Figure 8 contains a sample p-V diagram which shows a good agreement during the re-expansion and suction processes but some divergence during compression and discharge. The divergencies are similar to those obtained by Röttger (6) reproduced in Figure 9. The temperature of the gas in the cylinder, plotted with respect to crank angle was a few degrees lower when using the real gas equation model, so accounting for the larger mass of gas induced. The mass in the cylinder during re-expansion and compression should not change since valve and piston leakage were both set at zero, but due to accumulation errors in the iterative process when the step size was 1° crank angle, the mass varied slightly. The error would be reduced by reducing the step size. Figure 8 also includes the pressure in the cylinder during the suction and discharge phases, the two plenum chamber pressures, shown on the p-V diagram, having been assumed constant. The displacement diagrams for the suction and discharge valves indicate that the valves opened and closed slightly later when the real gas equation model was employed, as shown more clearly in Figure 3.

CONCLUSIONS

The simulation model using the real gas equation to relate the properties of refrigerant R12 gave a significant improvement in accuracy of the various parameters of interest to the designer only when the superheat at suction was small or the compressor pressure ratio was large. With high superheat at inlet, as in hermetic and semi-hermetic compressors, the refrigerant can be described adequately by an ideal gas equation.

Whether the real or ideal gas equation was used made negligible difference to the computer time required to run this particular model. The model computed the whole compressor cycle at small intervals of crank angle. In the Kerr model (2), the start and end of the re-expansion and compression processes are linked by an empirical index. The Kerr model was adequate, providing that appropriate indices are known, and was more economical of computer time.

NOMENCLATURE

A - Area
A_o - Maximum Valve Flow Area
C_d - Coefficient of Discharge
C_D - Pressure Drag Coefficient
F - Dimensionless Speed Ratio = ω/ω_n
g - Gravitational Acceleration
h - Specific Enthalpy
k - Spring Stiffness
m - Mass of Fluid
M - Effective Mass of Oscillating Valve System
p - Pressure
Q - Heat Transfer
R - Damping Coefficient
RPR - Ratio of Performance Ratios (Appendix A)
svc - Suction Valve Closing
svo - Suction Valve Opening
t - Time
T - Temperature
u - Specific Internal Energy
v - Specific Volume
V - Volume
$\bar{V}$ - Velocity
W - Work
y - Valve Lift
Y_o - Maximum Valve Lift
z - Height Above an Arbitrary Datum Level
α - Valve Lift Ratio = y/Y_o
γ - Isentropic Index
λ - Spring Preload
ω - Angular Speed of Crank
ω_n - Natural Frequency of Valve
θ - Crank Angle
Δp - Pressure Difference Across Valve

Subscripts

c - cylinder
d - discharge
i - inlet
I - ideal
o - outlet
R - real
s - suction
v - valve
1 - upstream
2 - downstream

APPENDIX A

VOLUMETRIC EFFICIENCY AND RATIO OF PERFORMANCE RATIOS

Volumetric efficiency was defined in four ways:

(a) A volumetric efficiency (theoretical) based on the ideal adiabatic cycle.

(b) An indicated volumetric efficiency (sv open) based on the period during which the suction valve is actually open.

(c) An actual volumetric efficiency (1) based on actual mass of gas induced per cycle.

(d) An actual volumetric efficiency (2) which accounts for throttling losses across the suction valve and valve blowby effects.

Thus

(a) $$\eta_{\text{vol theo.}} = \frac{\text{V indicated}}{\text{V swept}} = 1 - \frac{\text{V clearance}}{\text{V swept}}\left[\left(\frac{p_d}{p_s}\right)^{\frac{1}{\gamma}} - 1\right]$$

(b) $$\eta_{\text{vol ind.}} = \frac{\text{V(sv open)}}{\text{V swept}}$$

(c) $$\eta_{\text{vol actual 1}} = \frac{(m_{svc} - m_{svo})\, v_s}{\text{V swept}}$$

(d) $$\eta_{\text{vol actual 2}} = \eta_{\text{vol ind.}} - \text{throttling loss} - \text{blowby loss}$$

The values of (c) and (d) are close to one another.

The performance ratio (or specific pumping capacity) is defined as the mass throughput per unit work input, i.e.

Performance ratio (specific pumping capacity)

$$= \frac{\dot{m}}{\dot{W}} \quad (\text{lbm/hp hour})$$

The mass flow rates (theoretical and actual) were calculated from

$$\dot{m}_{\text{theo.}} = \eta_{\text{vol theo.}} \left[\frac{\text{V swept}}{v_s} \times \text{cycles/hr} \times \text{No of Cylinders}\right] \quad (\text{lbm/hr})$$

$$\dot{m}_{\text{act.}} = \eta_{\text{vol actual}} \left[\frac{\text{V swept}}{v_s} \times \text{cycles/hr} \times \text{No of Cylinders}\right] \quad (\text{lbm/hr})$$

The theoretical indicated work per cycle, $W_{\text{theo.}}$, was calculated by

$$W_{\text{theo.}} = \frac{n_1}{n_1 - 1} p_s V_1 \left[1 - \left(\frac{p_d}{p_s}\right)^{\frac{n_1 - 1}{n_1}}\right] + \frac{n_2}{n_2 - 1} p_s V_2 \left[\left(\frac{p_d}{p_s}\right)^{\frac{n_2 - 1}{n_2}} - 1\right]$$

where n_1 = expansion index of an ideal compressor cycle

n_2 = compression index of an ideal compressor cycle

V_1 = cylinder volume when the suction valve opens ideally

V_2 = cylinder volume when the suction valve closes ideally, i.e. when piston is at bottom dead centre

The actual indicated work per cycle, W_{actual}, was obtained by evaluating $\oint p_c \, d V_c$.

In consequence, the performance ratio (theoretical or actual indicated) may be calculated from

$$\frac{\dot{m}}{\dot{W}} .$$

To illustrate performance by a non dimensional parameter we introduce the ratio of performance ratios (RPR), (Fig. 5).

$$\text{RPR} = \frac{\text{actual performance ratio}}{\text{theoretical performance ratio}}$$

It can be shown that this criterion of performance simplifies the presentation of results by eliminating the effect of suction temperature (but not evaporator pressure, particularly at low values of compressor pressure ratio).

APPENDIX B

The basic equations used in the Martin-Downing form of equation of state may be written:

$$p = \frac{RT}{v - \beta} + \frac{A_2 + B_2 T + C_2 e^{(-KT/Tc)}}{(v - \beta)^2} + \frac{A_3 + B_3 T + C_3 e^{(-KT/Tc)}}{(v - \beta)^3}$$

$$+ \frac{A_4 + B_4 T + C_4 e^{(-KT/Tc)}}{(v - \beta)^4} + \frac{A_5 + B_5 T + C_5 e^{(-KT/Tc)}}{(v - \beta)^5}$$

$$+ \frac{A_6 + B_6 T + C_6 e^{(-KT/Tc)}}{e^{\alpha v}(1 + C_1 e^{\alpha v})}$$

$$h = aT + bT^2/2 + cT^3/3 + dT^4/4 - f/T + \phi pv + \phi$$

$$\left[\frac{A_2}{(v-\beta)} + \frac{A_3}{2(v-\beta)^2} + \frac{A_4}{3(v-\beta)^3} + \frac{A_5}{4(v-\beta)^4} + \frac{A_6}{\alpha}\left(\frac{1}{e^{\alpha v}} - C_1 \ln\left(\frac{C_1 e^{\alpha v}+1}{C_1 e^{\alpha v}}\right)\right)\right]$$

$$+ \phi\left[e^{-KT/Tc}(1 + KT/Tc)\left(\frac{C_2}{v-\beta} + \frac{C_3}{2(v-\beta)^2} + \frac{C_4}{3(v-\beta)^3} + \frac{C_5}{4(v-\beta)^4} + \frac{C_6}{\alpha e^{\alpha v}} - \frac{C_6 C_1}{\alpha}\ln\left(\frac{C_1 e^{\alpha v}+1}{C_1 e^{\alpha v}}\right)\right)\right]$$

$$+ \Delta h(\text{latent at } -40°F) - h(\text{saturated vapour at } -40°F)$$

$$s = a \ln T + bT + cT^2/2 + dT^3/3 - f/2T^2 + \phi R \ln(v-\beta)$$

$$-\phi\left[\frac{B_2}{v-\beta} + \frac{B_3}{2(v-\beta)^2} + \frac{B_4}{3(v-\beta)^3} + \frac{B_5}{4(v-\beta)^4} + \frac{B_6}{\alpha}\left(\frac{1}{e^{\alpha v}} - C_1 \ln\left(\frac{C_1 e^{\alpha v}+1}{C_1 e^{\alpha v}}\right)\right)\right]$$

$$+ \frac{\phi K e^{-KT/Tc}}{Tc}\left(\frac{C_2}{v-\beta} + \frac{C_3}{2(v-\beta)^2} + \frac{C_4}{3(v-\beta)^3} + \frac{C_5}{4(v-\beta)^4} + \frac{C_6}{\alpha e^{\alpha v}} - \frac{C_6 C_1}{\alpha}\ln\left(\frac{C_1 e^{\alpha v}+1}{C_1 e^{\alpha v}}\right)\right) +$$

$$\Delta s(\text{latent at } -40°F)/(-40) - s(\text{saturated vapour at } -40°F)$$

where A_2, A_3, A_4, A_5, A_6, B_2, B_3, B_4, B_5, B_6, C_1, C_2, C_3, C_4, C_5, C_6, K, α and β are the constants in the equations.

a, b, c, d, f are the constants in heat capacity of vapour equation

R is the universal gas constant
ϕ is the numerical factor depending on units
Tc is the critical temperature.

REFERENCES

1 MacLaren J F T - "A Review of Simple Mathematical Models of Valves in Reciprocating Compressors" Proc. 1972 Purdue Compressor Technology Conference, p 180

2 MacLaren J F T and Kerr S V - "An Analytical and Experimental Study of Self-acting Valves in a Reciprocating Air Compressor" - Proc. I. Mech. E. Conference, Industrial Reciprocating and Rotary Compressor Design and Operational Problems, London, October 1970, Paper No 3 (Proc. I. Mech. E, Vol 184, Part 3R, 1969-70, pp 24 - 33)

3 Soedel W - "Introduction to Computer Simulation of Positive Displacement Type Compressors" - Short Course Text, Purdue University, 1972

4 Prakash R and Singh R - "Mathematical Modeling and Simulation of Refrigerating Compressors" - Proc. 1974 Purdue Compressor Technology Conference, p 274

5 Riemer D H, Jacobs H R and Boehm R F - "A Computer Program for Determining the Thermodynamic Properties of Freon Refrigerants" University of Utah

6 Röttger W - "Digitale Simulation von Kaltekompressoren unter Verwendung Realer Zustandsgleichungen", PhD Thesis, Hanover 1975

7 MacLaren J F T and Tramschek A B - "Prediction of Valve Behaviour with Pulsating Flow in Reciprocating Compressors" - Proc. 1972 Purdue Compressor Technology Conference, p 203

8 MacLaren J F T, Kerr S V, Tramschek A B and Sanjines O A - "A Model of a Single Stage Reciprocating Gas Compressor accounting for Flow Pulsation", Proc. 1974 Purdue Compressor Technology Conference, p 144

9 Costagliola M - "The Theory of Spring-Loaded Valves for Reciprocating Compressors" - J. App. Mech., Dec 1950 17,4, p 415